

## **Timeless couples G quadruplex detection with processing by DDX11 during DNA replication**

Leticia Koch Lerner<sup>1&</sup>, Sandro Holzer<sup>2&</sup>, Mairi L. Kilkenny<sup>2</sup>, Pierre Murat<sup>1</sup>, Saša Šviković<sup>1</sup>, Davide Schiavone<sup>1</sup>, Alice Bittleston<sup>2</sup>, Joseph D. Maman<sup>2</sup>, Dana Branzei<sup>3</sup>, Katherine Stott<sup>2</sup>, Luca Pellegrini<sup>2\*</sup> and Julian E. Sale<sup>1\*</sup>

<sup>1</sup> MRC Laboratory of Molecular Biology, Francis Crick Avenue, Cambridge, CB2 0QH, UK

<sup>2</sup> Department of Biochemistry, University of Cambridge, Cambridge, CB2 1GA, UK

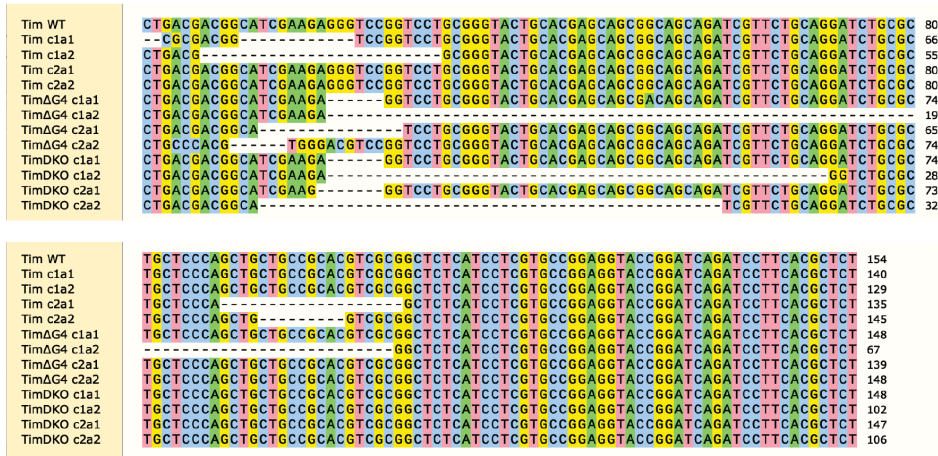
<sup>3</sup>IFOM, Fondazione Italiana per la Ricerca sul Cancro, Institute of Molecular Oncology, Milan, 20139, Italy

\* to whom correspondence should be addressed: [jes@mrc-lmb.cam.ac.uk](mailto:jes@mrc-lmb.cam.ac.uk) or [lp212@cam.ac.uk](mailto:lp212@cam.ac.uk)

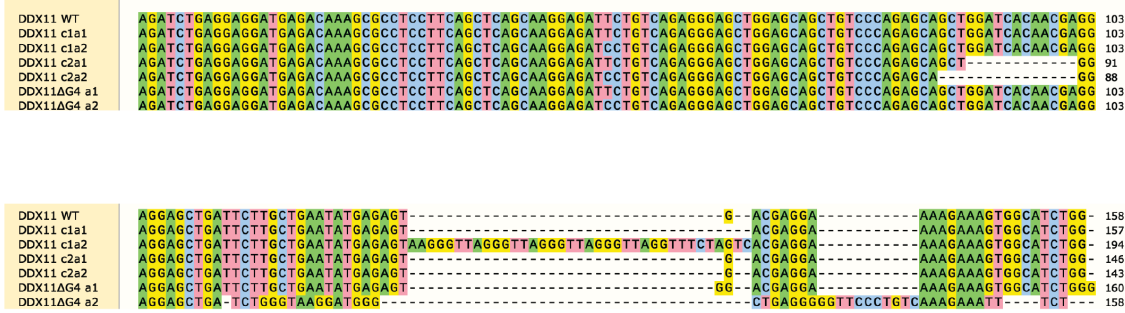
& equal contribution

**SUPPLEMENTARY INFORMATION**

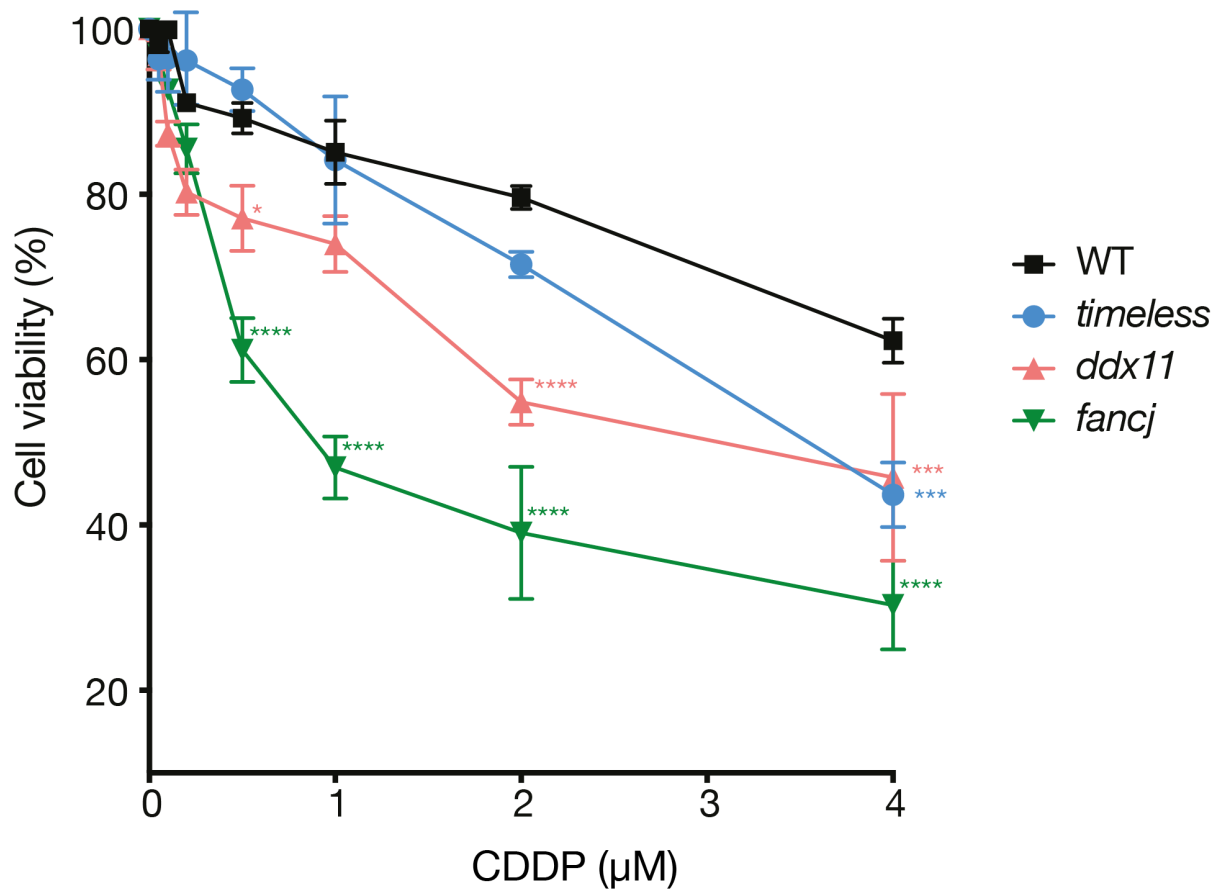
a



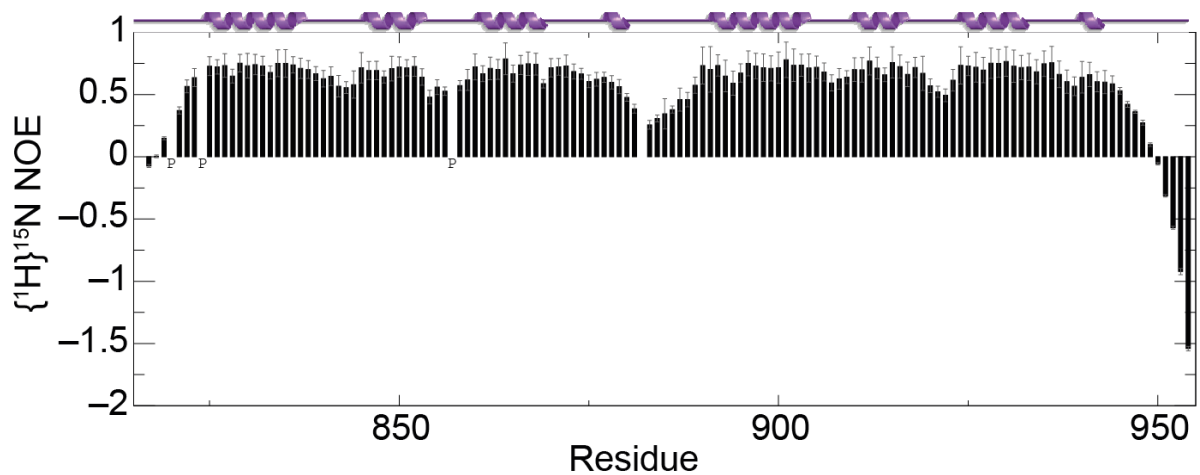
b



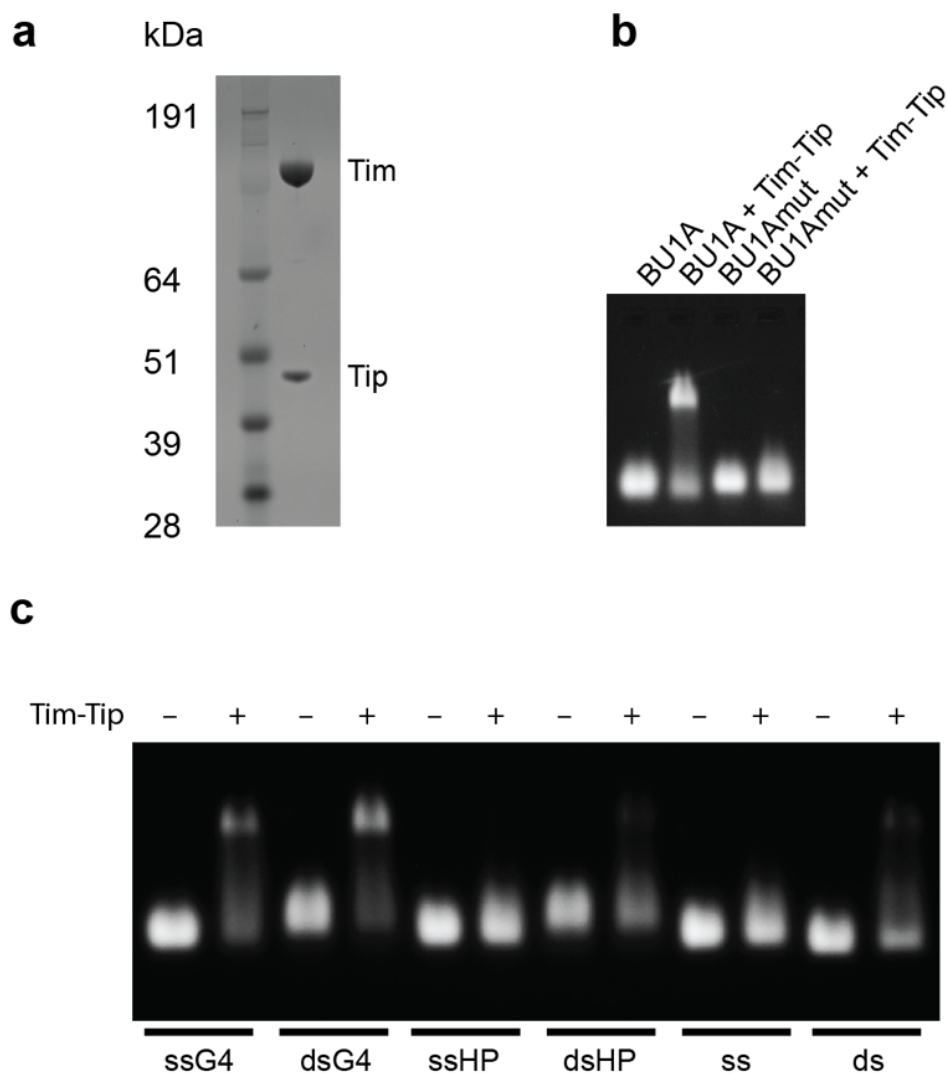
**Supplementary Fig. 1. CRISPR-Cas9 induced deletions in *TIMELESS* and *DDX11*.** A. Aligned sequences of Exon 1 of the chicken *TIMELESS* locus showing the disruptions induced in the different clones used in this study. a1 and a2 refer to the two alleles. Note the telomeric repeat inserted in clone DDX11 c1a2. All disruptions lead to loss of frame.



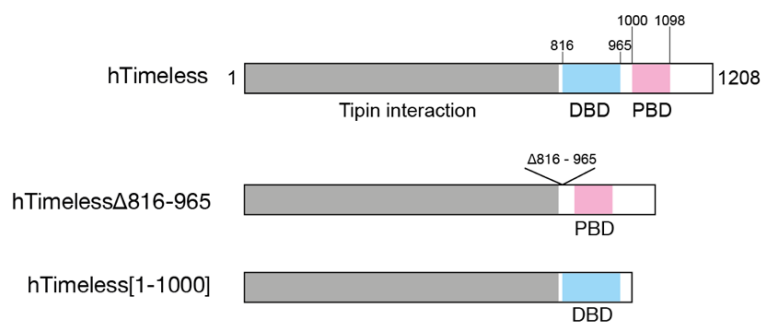
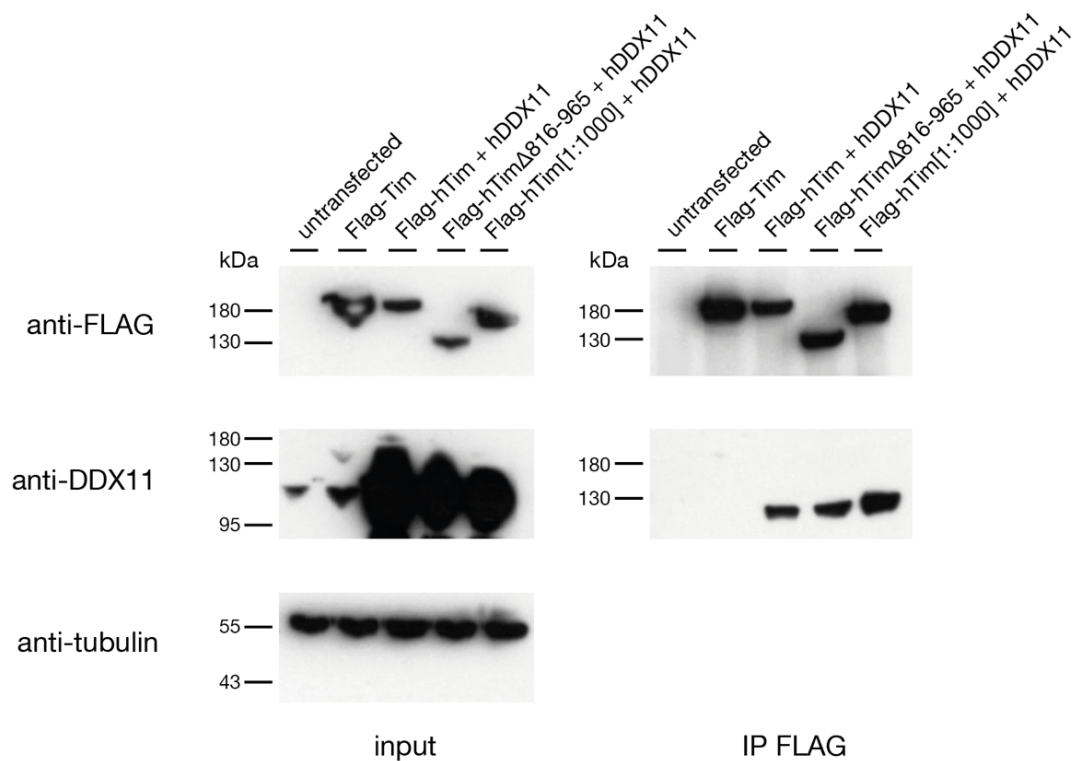
**Supplementary Fig. 2. Sensitivity of wild type (WT), *timeless*, *ddx11* and *fancj* DT40 mutants to cisplatin (CDDP).** Cell viability, assessed by MTS assay, of DT40 wild type, *ddx11*, *timeless*, *fancj*, after 72 h in presence of cisplatin at the indicated doses. The values represent the means (error bars indicate SD) of two independent experiments performed in triplicate. \* p < 0.05, \*\*\* p < 0.001 and \*\*\*\* p < 0.0001; one-way ANOVA compared to the wild type.



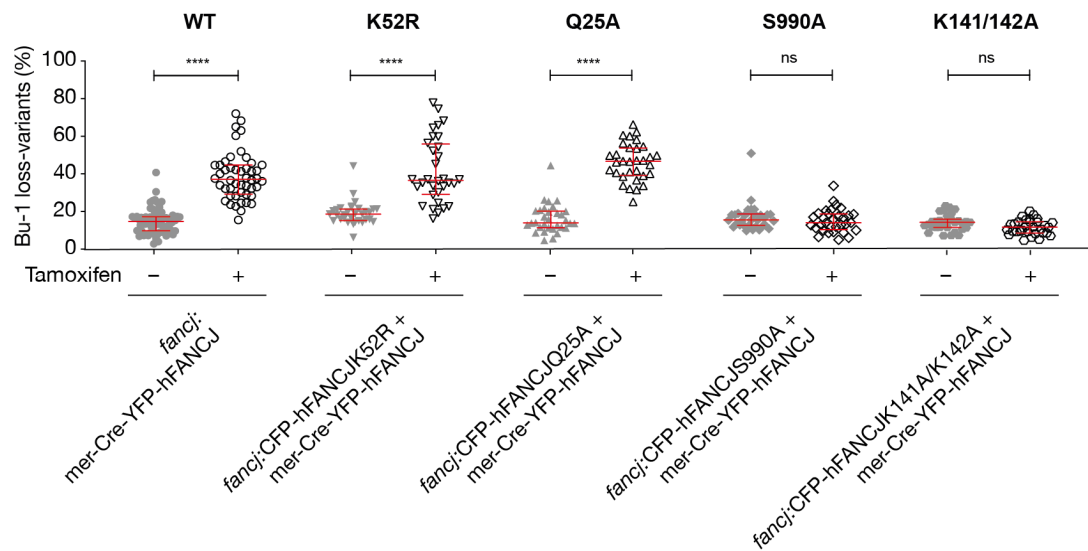
**Supplementary Fig. 3. Backbone dynamics of Timeless 816-954.**  $^1\text{H}^{15}\text{N}$  heteronuclear nuclear Overhauser enhancement (NOE) values for the inter-domain linker region (residues 881-890) showed evidence of increased motions (NOE < 0.6) on a time scale faster than the overall tumbling rate. The linker is therefore flexible and confers independent mobility on the domains, which leads to a lack of global convergence of the NMR ensemble. Proline residues that lack  $^1\text{H}^{\text{N}}$  are marked 'P'; the  $^1\text{H}^{\text{N}}$  of residue 882 was not detected due to conformational exchange broadening. Secondary structure from PDBsum.



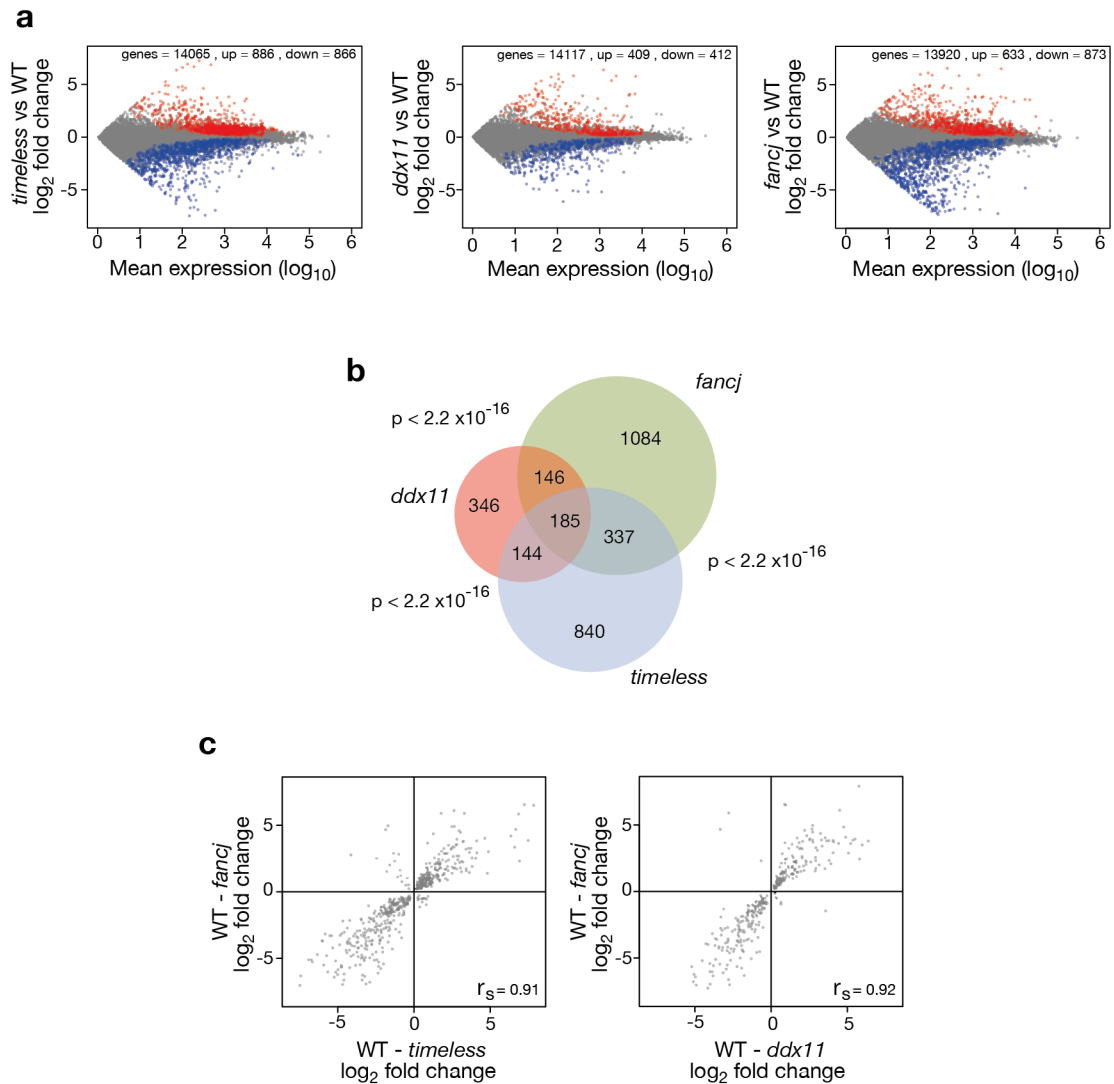
**Supplementary Fig. 4. The Timeless-Tipin complex shows a preference for binding G-quadruplex DNA structures.** A Coomassie-stained SDS-PAGE gel of purified Timeless-Tipin complex. B Electrophoretic mobility shift assay (EMSA) showing the binding of Timeless-Tipin to G-quadruplex sequence BU1A+3.5. Mutation of the G-quadruplex sequence (BU1A+3.5mut) disrupts Timeless-Tipin binding (see Supplementary Table 2 for sequence details). Timeless-Tipin and DNA are both present at a final concentration of 5  $\mu$ M. C EMSA showing the binding of Timeless-Tipin to G-quadruplex sequences (ssG4, dsG4) but not single-stranded DNA (ss), double-stranded DNA (ds) or hairpin-containing sequences (ssHP, dsHP). Timeless-Tipin and DNA are both present at a final concentration of 5  $\mu$ M.



**Supplementary Fig. 5. The C-terminus of Timeless is not required for its interaction with DDX11.** HEK293T cells were transiently transfected with a plasmid encoding Flag-hTimeless, or co-transfected with plasmids encoding hDDX11 and Flag-Timeless or with Timeless mutated to delete the DNA binding domain ( $\Delta$ DBD: deletion of region S816-S965) or PARP binding domain (PARP\*: truncation at V1000). 24 h after transfection, whole cell extracts were subjected to immuno-precipitation with anti-Flag magnetic beads. Western Blot analyses were performed to detect overexpressed DDX11 protein in the pulled down samples using a specific antibody. Upper panel: Input and pulled down samples transfected with different Timeless constructs detected with an anti-Flag antibody. Bottom panel: Input and pulled down samples transfected with different Timeless constructs detected with an anti-DDX11 antibody. Tubulin was used as a loading control for the input samples.



**Supplementary Fig. 6. The catalytic activity of FANCJ is required for its role in suppressing G4-induced instability of *BU-1* expression.** Fluctuation analysis for the generation of Bu-1 loss variants in an inducible system to study FANCJ function (see Methods for full details). Briefly FANCJ-deficient DT40 cells are rescued with two transgenes, one encoding the wild type protein, the other the mutant in question. The wild type transgene is flanked by loxP sites and can be deleted by expression of Cre recombinase, induced by treatment of cells with tamoxifen. The K52R and Q25A mutants of FANCJ both disrupt the helicase activity of the enzyme <sup>1,2</sup>. S990A disrupts the interaction of FANCJ with BRCA1, which is important for the role of FANCJ in homologous recombination <sup>3</sup>. K141/142A disrupts the interaction of FANCJ with MutL $\alpha$ , which is needed for efficient interstrand crosslink repair <sup>4</sup>.



**Supplementary Fig. 7. Gene expression dysregulation in *timeless* and *ddx11* DT40 cells.**

**a.** Dysregulated genes in *timeless* (left panel), *ddx11* (centre panel) and *fancj* (right panel) mutants relative to wild type. All genes with  $> 1$  transcript per million in both conditions are plotted. Significantly ( $p \geq 0.95$ ) upregulated genes shown in red; downregulated in blue **b.** Venn diagram showing the overlap in genes deregulated in *timeless*, *ddx11* and *fancj* relative to wild type.  $p < 2.2 \times 10^{-16}$  for each pairwise comparison (Fisher hypergeometric distribution). **c.** Correlation of magnitude and direction of change of genes dysregulated (relative to wild type) in *fancj* vs. *timeless* (left panel) and *ddx11* (right panel) DT40 cells.  $r_s$  (Spearman rho) is shown for each correlation.



**Supplementary Table 1.** Oligos used for molecular cloning, site-directed mutagenesis and CRISPR/Cas9 gene disruption

Identifier	5'-3' DNA Sequence
hTim $\Delta$ DBD-D965-ClaI-GA-Fw	AGATGACTGAGGGCTATGGCTCCCTGGATGACAGGTC TTCCATCGATTTTTGCCAGGAAGATCTGGAAGAAGAG G
hTim $\Delta$ DBD-S816-ClaI-GA-Rev	TTCCTCAGGCAGGTTTTCTCTTCTTCCAGATCTTCTG GCAAAAATCGATGGAAGACCTGTCATCCAGGGAGCC
hTimPBDtrunc-pcDNA3.1-bGH-TGA-NotI-GA-Fw	CAAGTCCAGGGTAGCTTAGTCTGAGCGGCCGCTCGAG TCTAGAGGGCCCTTCG
hTimPBDtrunc-NotI-GA Rev	CCCTCTAGACTCGAGCGGCCGCTCAGACTAAGCTACC CTGGACTTGTCTGC
hTimC-tertrunc-pcDNA3.1-bGH-TGA-NotI-GA-Fw	GCTCCCTGGATGACAGGTCTTCTGAGCGGCCGCTCG AGTCTAGAGGGCCCTTCG
hTimC-tertrunc-S816-NotI-GA-Rev	AAGGGCCCTCTAGACTCGAGCGGCCGCTCAGGAAGAC CTGTTCATCCAGGGAGCC
hFANCJ K52R A155G Fw	AAGTAAGGCTAAGCTTCTTCCACTTCTGTGGGAC
hFANCJ K52R A155G Rev	GTCCCACAGGAAGTGGAAGAAGCTTAGCCTTACTT
cDDX11 CRISPR gRNA top	CACCGTGCTGAATATGAGAGTGACG
cDDX11 CRISPR gRNA bottom	AAACCGTCACTCTCATATTCAGCAC
cTim CRISPR (KO) gRNA top	CACCGCGACGGCATCGAAGAGGGTC
cTim CRISPR (KO) gRNA bottom	AAACGACCCTTTCGATGCCGTCGC

cTim CRISPR (C-ter truncation) gRNA top	CACCGACTTGTCGTCGTGTGCGGCC
cTim CRISPR (C-ter truncation) gRNA top	AAACGGCCGCACACGACGACAAGTC

**Supplementary Table 2.** DNA sequences used in Timeless DNA-binding experiments

Identifier	5'-3' DNA sequence (secondary structure forming elements are highlighted in red)
ssGQ	<b>6FAM-</b> ACGAGAGCTAGCACATTTTGA <b>GGGTGGGTAGGGTGGG</b> TAATTTTCACGTAGAACCTGT
dsGQ	ssGQ+ ACAGGTTCTACGTGATTTTTTTTTTTTTTTTTTTTTTTTTTTTTTTTTTTTGTGCTAGCTCTCGT
ssHP	<b>6FAM-</b> ACGAGAGCTAGCACATTT <b>TTGAGGCTGCG</b> TTT <b>CGCAGCCTCA</b> ATTTTCACGTAGAACCTGT
dsHP	ssHP+ ACAGGTTCTACGTGATTTTTTTTTTTTTTTTTTTTTTTTTTTTTTTTTTTTGTGCTAGCTCTCGT
ss	<b>6FAM-</b> ACGAGAGCTAGCACATTTT <b>GAGTGTCAGTAGCGTCTGTA</b> ATTTTCACGTAGAACCTGT
ds	ss+ ACAGGTTCTACGTGAAAATTACAGACGCTACTGACACTCAAATGTGCTAGCTCTCGT
BU1 +3.5 <sup>5</sup>	<b>6FAM-</b> AGCTAGCACATTTTAA <b>GGGCTGGGTGGGT</b> GTCTGTCA <b>GGGCTGGG</b> TTTTTCACGTAGAA
BU1 +3.5mut <sup>5</sup>	<b>6FAM-</b> AGCTAGCACATTTTAA <b>GTTCTGTTTGTTG</b> CTGTCAAGTTCTGTTTTTTTCACGTAGAA
2JPZ <sup>6</sup>	<b>6FAM-TTAGGGTTAGGGTTAGGGTTAGGGTT</b>
1XAV <sup>7</sup>	<b>6FAM-TGAGGGTGGGTAGGGTGGGTAA</b>
G4#2 <sup>5</sup>	<b>6FAM-TAATGGGTTTGGGTTTGGGTTTGGGT</b>
G4#4 <sup>5</sup>	<b>6FAM-TAATTTTGGGTGGGTGGGTGGGTTT</b>
2O3M <sup>8</sup>	<b>6FAM-TAAGGGAGGGCGCTGGGAGGAGGG</b>
Bcl2Mid <sup>9</sup>	<b>6FAM-ATAGGGCGCGGGAGGAAGGGGGCGGG</b>
ρ-globin <sup>10</sup>	<b>6FAM-TAAGGGGAGTAAAAGGGAGCGGGGTGCTGGG</b>

**Supplementary Table 3. Data collection and refinement statistics for Tim DBD C-term (residues 883-947).**

*Data collection*

Wavelength	0.9686 Å
Resolution range (Å)	31.46 - 1.15 (1.191 - 1.15)
Space group	P6 <sub>5</sub>
Unit cell	55.407 55.407 41.659 90 90 120
Total reflections	104424 (3064)
Unique reflections	25072 (1920)
Multiplicity	4.2 (1.6)
Completeness (%)	96.33 (74.84)
Mean I/sigma(I)	6.82 (1.36)
Wilson B-factor	11.30
R-merge	0.1377 (0.4873)
R-meas	0.1543 (0.6505)
R-pim	0.06851 (0.4274)
CC1/2	0.975 (0.464)
CC*	0.994 (0.796)

*Refinement*

Reflections used in refinement	24985 (1922)
Reflections used for R-free	1267 (101)
R-work	0.1280 (0.2681)
R-free	0.1548 (0.3632)
CC(work)	0.973 (0.809)

CC(free)	0.963 (0.769)
Number of non-hydrogen atoms	659
macromolecules	527
solvent	132
Protein residues	62
RMS(bonds)	0.008
RMS(angles)	0.96
Ramachandran favored (%)	96.67
Ramachandran allowed (%)	3.33
Ramachandran outliers (%)	0.00
Rotamer outliers (%)	0.00
Clashscore	1.86
Average B-factor	17.72
macromolecules	14.14
solvent	32.01

Statistics for the highest-resolution shell are shown in parentheses.

**Supplementary Table 4.** Summary of the restraints used in the calculation of the Timeless 816-954 structure and characterisation of the ensemble of energy-minimised structures.

<i>NOE upper distance limits</i>		
Total		4730
Ambiguous		1912
Unambiguous		2818
<i>Dihedral angle constraints</i>		
Total		278
<i>Residual NOE violations (Å)</i>		
Number $\geq 0.5$		0
Number $\geq 0.1$		117
<i>Residual angle violations (deg.)</i>		
Number $\geq 2.0$		0
<i>Energies (kcal mol<sup>-1</sup>)</i>		
Total		-4691 $\pm$ 40
van der Waals		-1348 $\pm$ 40
Electrostatic		-5207 $\pm$ 53
<i>Ramachandran statistics (% residues)</i>		
Core regions		83.7
Allowed regions		16.3
Generously allowed regions		0
Disallowed regions		0
<i>r.m.s.d. from ideal geometry</i>		
Bond lengths (Å)		0.0052 $\pm$ 0.0002
Bond angles (deg.)		0.660 $\pm$ 0.008
<i>r.m.s.d. to mean coordinates (Å)</i>		
	<i>Backbone</i>	<i>Heavy atoms</i>
Protein (824-880)	0.494	0.580
Protein (891-944)	0.487	0.527
For the analysis, 20 water-refined, energy-minimised structural conformations were used. Ramachandran statistics were calculated using PDBsum.		

## Supplementary References

1. Cantor, S. B. et al. BACH1, a novel helicase-like protein, interacts directly with BRCA1 and contributes to its DNA repair function. *Cell* **105**, 149-160 (2001).
2. Wu, Y. et al. The Q motif of Fanconi anemia group J protein (FANCI) DNA helicase regulates its dimerization, DNA binding, and DNA repair function. *J Biol Chem* **287**, 21699-21716 (2012).
3. Xie, J. et al. Targeting the FANCI–BRCA1 interaction promotes a switch from recombination to pol $\eta$ -dependent bypass. *Oncogene* **29**, 2499-2508 (2010).
4. Peng, M. et al. The FANCI/MutL $\alpha$  interaction is required for correction of the cross-link response in FA-J cells. *EMBO J* **26**, 3238-3249 (2007).
5. Schiavone, D. et al. Determinants of G quadruplex-induced epigenetic instability in REV1-deficient cells. *The EMBO Journal* **33**, 2507-2520 (2014).
6. Dai, J., Carver, M., Punchihewa, C., Jones, R. A. & Yang, D. Structure of the Hybrid-2 type intramolecular human telomeric G-quadruplex in K<sup>+</sup> solution: insights into structure polymorphism of the human telomeric sequence. *Nucleic Acids Res* **35**, 4927-4940 (2007).
7. Ambrus, A., Chen, D., Dai, J., Jones, R. A. & Yang, D. Solution structure of the biologically relevant G-quadruplex element in the human c-MYC promoter. Implications for G-quadruplex stabilization. *Biochemistry* **44**, 2048-2058 (2005).
8. Phan, A. T., Kuryavyi, V., Burge, S., Neidle, S. & Patel, D. J. Structure of an unprecedented G-quadruplex scaffold in the human c-kit promoter. *J Am Chem Soc* **129**, 4386-4392 (2007).
9. Dai, J., Chen, D., Jones, R. A., Hurley, L. H. & Yang, D. NMR solution structure of the major G-quadruplex structure formed in the human BCL2 promoter region. *Nucleic Acids Res* **34**, 5133-5144 (2006).
10. Sarkies, P., Reams, C., Simpson, L. J. & Sale, J. E. Epigenetic instability due to defective replication of structured DNA. *Mol Cell* **40**, 703-713 (2010).